Available online at www.eccomasproceedia.org
Eccomas Proceedia COMPDYN (2025) 1167-1179

ECCOMAS
Proceedia

COMPDYN 2025
10th ECCOMAS Thematic Conference on
Computational Methods in Structural Dynamics and Earthquake Engineering
M. Papadrakakis, M. Fragiadakis (eds.)
Rhodes Island, Greece, 15-18 June 2025

MODEL REDUCTION STRATEGY FOR THE DYNAMIC ANALYSIS OF PLATES WITH A NEARLY PERIODIC ARRAY OF CIRCULAR ACOUSTIC BLACK HOLES

V. Denis and J.-M. Mencik

INSA Centre Val de Loire, Université d'Orléans, Université de Tours, Laboratoire de Mécanique Gabriel Lamé, Rue de la Chocolaterie, 41000 Blois, France
e-mail: {vivien.denis, jean-mathieu.mencik}@insa-cvl.fr

Abstract. *The concept of acoustic black hole (ABH) refers to bending stiffness decrease and added damping to localize and efficiently dissipate flexural vibrations in thin structures. For plate-like structures, a ABH typically takes the form of a circular pit whose thickness decreases as a power-law with the distance to the center. The central region has a very small residual thickness, and it is covered by a damping layer. While being inefficient at low frequencies, ABHs can drastically lowered the resonant behavior of a host structure at high frequencies (after a certain cut-on frequency). 2D-periodic arrays of circular ABHs embedded in a host structure can be involved, where the periodicity property is used to create low frequency band gaps. For instance, a small mass can be added to the center of each circular ABH to create resonant band gaps. Besides the analysis of structures with periodic arrays of ABHs, nearly periodic structures will be explored in this paper to see whether the lack of periodicity can be detrimental to create band gaps, or, on the contrary, if this can be used to enlarge band gaps. In the case of a periodic array of circular ABHs with central masses, near-periodicity can result from manufacturing imperfections of the ABH thicknesses, or slight variations of the central masses. Those nearly-periodic structures can be seen as assemblies of different substructures (i.e., structure cells encompassing an ABH) subjected to parametric changes. For nearly-periodic structures built from finite element models of substructures with many degrees of freedom, parametric model order reduction strategies can be used to reduce the computational costs of the forced response simulations. In this paper, an interpolation strategy will be explored to approximate the reduced matrices of substructures over parametric spaces. This circumvents the need for computing the component mode bases, and the reduced matrices, many times for investigating different parametric changes. An enhanced version of this strategy is proposed here, which includes interface reduction and basis enrichment techniques. Numerical experiments are carried out on a plate with circular ABHs.*

Keywords: Structural Dynamics, Vibration, Acoustic Black Holes, Model Reduction, Component Mode Synthesis, Periodicity

ISSN:2623-3347 © 2025 The Authors. Published by Eccomas Proceedia.
Peer-review under responsibility of the organizing committee of COMPDYN 2025.
doi: 10.7712/120125.12480.25380

1 INTRODUCTION

In vibration control of thin structures, property gradients can be used to promote energy localization and dissipation. This is the principle behind acoustic black hole (ABH) [1, 2], where a gradual power-law-based decrease of the thickness of a plate (or beam), combined with a local increase of the damping (such as adding a viscoelastic layer), allows localization and efficient dissipation of flexural waves.

Part of the recent literature focused on embedding periodic arrays of ABHs in thin structures. In [3], Zhu & Semperlotti studied phononic thin plates embedding 2D circular ABHs, and the related dispersion properties of waves. Aklouche [4] investigated the possibility to create low frequency band gaps using rectangular and triangular ABH lattices. "Ultrawide" band gaps in phononic beams with double leaf ABH were found by Tang & Cheng [5]. The authors also investigated the 1D propagation of waves in plates embedding ABHs [6]. Zhao [7] conducted studies on structures with an array of circular ABHs, disregarding the analysis of the periodicity properties induced by this array. Deng et al. [8] studied evanescent waves in a beam embedding pillar-type ABH. Also, Deng et al. [9] discussed the damping effect on the determination of the complex dispersion curves in structures with 2D arrays of circular ABHs. Finally, the dispersion properties and band gaps induced by 1D arrays of circular ABHs were studied by Han et al. [10].

Thin structures embedding a periodic array of circular ABHs can be seen as periodic structures with identical substructures representing unit cells with an ABH. Usually, the substructures are described from finite element (FE) meshes with moderately high numbers of degrees of freedom (DOFs) to obtain accurate results. Component mode synthesis techniques seem to constitute efficient model order reduction strategies to alleviate the computational cost required to perform heavy simulations, i.e., to predict the dynamic response of periodic structures with large-sized substructure models. In particular, the Craig-Bampton (CB) method consists in reducing the internal DOFs of a substructure using static modes and a reduced set of fixed interface modes [11]. For periodic structures, the CB method involves computing the component modes (static, fixed interface) of a substructure, and projecting the mass, damping and stiffness matrices of this substructure onto the space spanned by these component modes (Galerkin projection). Since the substructures are all identical, these numerical steps only need to be considered once. Next, the reduced substructure matrices (i.e., once projected onto the space of the component modes) can be assembled in a standard way to obtain a reduced model of a whole periodic structure. Eventually, an interface reduction — where the interface DOFs between the substructures are expressed from a reduced set of interface modes [12] — can be considered to further reduce the computational cost of the FE simulations.

Nearly periodic structures consist of different substructures with parameter-dependent FE models, which are described from different component modes and different reduced matrices. This requires computing the component modes and the reduced matrices many times, which results in highly consuming repetitive steps, and makes the CB method quite inefficient. To solve this issue, an interpolation strategy can be proposed as in [12, 13]. For a nearly periodic structure, this consists in computing the reduced substructure matrices at some points in a parametric space, and interpolating the reduced matrices between these points using standard interpolation functions. Also, with this approach, the interface DOFs (between the substructures) are expressed using the interface modes of the equivalent purely periodic structure. In this sense, the interface modes do not need to be recomputed at every new substructure change. In [14], two updates of this interpolation strategy have been proposed, focused on predicting accurate response functions of nearly periodic structures at high frequencies. This consists in adding high-order static modes into the component basis of a substructure, and adding static correction terms into the interface mode basis to account for the effect of the parametric changes of the substructures.

In this paper, the dynamic behavior of nearly periodic structures is investigated in the context of ABH. In Sec.2, some basics about the ABH models are given; also, preliminary results about wave propagation in plates with periodic arrays of circular ABHs are given. In Sec. 3, the key steps of the interpolation strategy, including the basis enrichment technique based on high-order static modes (as explained earlier), are discussed. In Sec. 4, numerical results are proposed, and the effect of periodic and nearly periodic arrays of ABHs on the vibration control of plates is discussed.

2 ACOUSTIC BLACK HOLE

2.1 Analytical model

The main idea behind ABH is to consider a thin structure with a gradient of properties. In the case of a thin plate with variable thickness, the equation of motion for the transverse displacement $w = w(x, y, t)$ writes

$$\rho h(x,y)\ddot{w} + \Delta(D(x,y)\Delta w) - (1-\nu)L(D(x,y), w) = p, \tag{1}$$

where ρ and ν are the density and the Poisson's ratio of the plate (respectively), $h(x, y)$ is the thickness, $D(x, y) = Eh(x, y)^3/12(1 - \nu^2)$ is the bending stiffness (E being the Young's modulus), $p = p(x, y, t)$ is the force distribution and $L(f, g) = f_{,xx}g_{,yy} + f_{,yy}g_{,xx} - 2f_{,xy}g_{,xy}$. The thickness is described as a power-law in a circular zone of radius R centered at the origin:

$$h(x,y) = \begin{cases} h_0 & \text{if} \quad x^2 + y^2 \geq R, \\ h_{\min} + \frac{(h_0 - h_{\min})}{R^m}(x^2+y^2)^{m/2} & \text{if} \quad x^2 + y^2 < R, \end{cases} \tag{2}$$

where h_0 is the thickness in the region away from the ABC, $h_{\min}$ is the minimum thickness, and m is the exponent of the power-law. A loss factor η may be included to describe a complex bending stiffness. Likewise, a circular damping layer (radius R_l and loss factor η_l) may be taken into account using a compound law [15, 16] in the central ABH region to obtain a complex bending stiffness.

2.2 Wave propagation in plate with a periodic array of circular ABHs

The analysis of periodic arrays of ABHs has been conducted in [4]. A key point is that, for periodic arrays of circular ABHs, the addition of a small mass at the center of each ABH opens a narrow resonant band gap, whose central frequency corresponds to the frequency of a local "piston" mode of the ABH substructure (i.e., when the center of each ABH strongly vibrates). Such a ABH configuration will be investigated throughout the present paper. For instance, a preliminary analysis conducted via COMSOL Multiphysics can be done to compute the band diagram in a periodic structure with 0.3 × 0.3 m^2 steel cells modeled using plate elements, when each cell embeds a ABH with a quadratic profile, and with a central mass of 10 g (see Figs. 2(a,b)). The nominal thickness is $h_0 = 2$ mm and the thickness in the central region is $h_{\min} = 50$ μm. The computed band diagram is displayed in Fig. 1, which shows a narrow band gap around 39 Hz that corresponds to the local piston mode, as expected. Band gaps occur provided the structure is purely periodic. A nearly periodic structure could involves slightly perturbating the local masses of the ABHs, and, therefore, affecting the band gap effect.

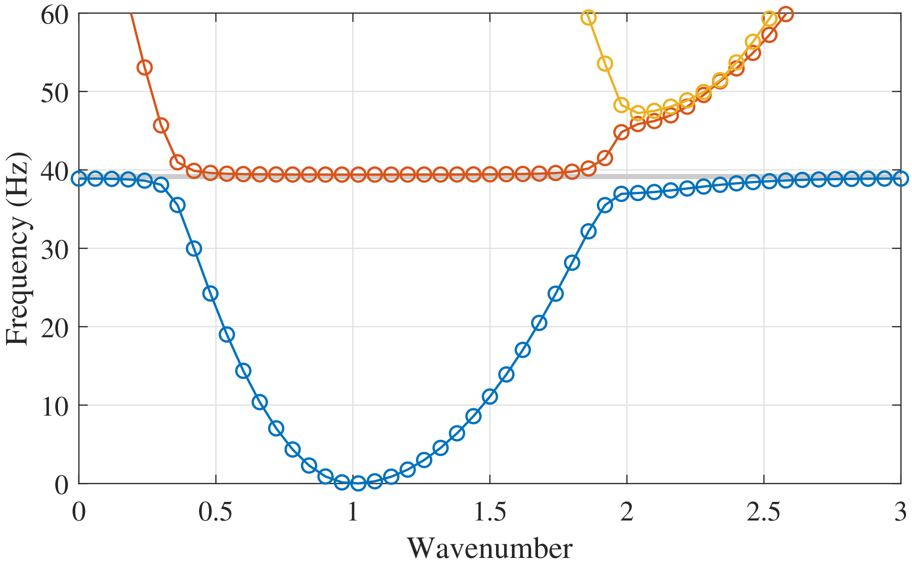

Figure 1: Band diagram for a periodic structure made of 0.3 × 0.3 m ABH cell with a 10 g central mass. The thin gray shaded area indicates the resonant band gap.

3 MODEL REDUCTION STRATEGY

3.1 FE model of ABH substructures

An ABH substructure with variable thickness can be meshed using DKT triangular plate elements [17]. A DKT triangular element has 3 nodes with 3 DOFs per node, say $\mathbf{u}_i = [w_i \, \beta_{xi} \, \beta_{yi}]^T$ with w_i the transverse displacement, and $\beta_{xi} = -w_{i,x}$ and $\beta_{yi} = -w_{i,y}$ the rotations (for each node i). For the sake of clarity, it is reminded that the displacements and curvatures in a plate element e are approximated through interpolation functions $\mathbf{N}(x, y)$ and $\mathbf{B}(x, y)$ as:

$$w(x, y) = \mathbf{N}(x, y) \, \mathbf{u}^e, \tag{3}$$

and

$$-[w_{,xx} \, w_{,yy} \, 2w_{,xy}]^T = [\beta_{x,x}(x, y) \, \beta_{y,y}(x, y) \, \beta_{x,y}(x, y) + \beta_{y,x}(x, y)]^T = \mathbf{B}(x, y) \, \mathbf{u}^e, \tag{4}$$

where $\mathbf{u}^e = [(\mathbf{u}_1^e)^T (\mathbf{u}_2^e)^T (\mathbf{u}_3^e)^T]$. Within this framework, the elementary mass and stiffness matrices write:

$$\mathbf{M}^e = \int_{\Omega^e} \rho h(x, y) \, \mathbf{N}^T \, \mathbf{N} \, \mathrm{d}S, \tag{5}$$

and

$$\mathbf{K}^e = \int_{\Omega^e} \mathbf{B}^T \, D(x, y) \begin{bmatrix} 1 & \nu & 0 \\ \nu & 1 & 0 \\ 0 & 0 & (1-\nu)/2 \end{bmatrix} \mathbf{B} \, \mathrm{d}S, \tag{6}$$

where Ω^e is the domain of the element e. Three hammer points are used for the numerical integration of the elementary matrices, which allows a variable thickness to be taken into account within an element. The FE mesh of an ABH substructure can be obtained using the MATLAB mesh generator `distmesh` [18], and a standard FE assembly procedure. In this case, an adaptive FE mesh is required within the ABH region to conform with the varying wavelength in this region. For instance, a FE mesh of an ABH substructure containing about 3100 elements, and

9300 DoFs, is shown in Fig. 2(a). The dynamic equation of a substructure, in the frequency domain, writes:

$$(-\omega^2\mathbf{M} + \mathbf{K}^\star)\mathbf{u} = \mathbf{F}, \tag{7}$$

where $\mathbf{u}$ is the displacement/rotation vector, $\mathbf{F}$ is the force/moment vector, ω is the frequency, $\mathbf{M}$ is the mass matrix, and $\mathbf{K}^\star$ is the complex stiffness matrix. In this case, damping effects can be introduced by means of a loss factor. This yields a complex bending stiffness $D^*(x,y) = D(x,y) + \mathrm{i}D''(x,y)$ [15, 16], and therefore a complex stiffness matrix:

$$\mathbf{K}^\star = \mathbf{K} + \mathrm{i}\mathbf{K}''. \tag{8}$$

Finally, a central mass m^s can be added to the substructure by modifying the mass matrix as:

$$\mathbf{M} \leftarrow \mathbf{M} + (\mathbf{L}^s_m)^T m^s \mathbf{L}^s_m \tag{9}$$

where $\mathbf{L}^s_m$ is a localization matrix.

3.2 Reduced order models of substructures

A reduced substructure model can be obtained using the CB method. Within the CB framework, the displacement/rotation vectors $\mathbf{u}_{\mathrm{B}}$ and $\mathbf{u}_{\mathrm{I}}$, for the internal and boundary DOFs, are approximated as:

$$\mathbf{u} = \begin{bmatrix} \mathbf{u}_{\mathrm{B}} \\ \mathbf{u}_{\mathrm{I}} \end{bmatrix} \approx \begin{bmatrix} \mathbf{I} & \mathbf{0} \\ \mathbf{X}_{\mathrm{st}} & \widetilde{\mathbf{X}} \end{bmatrix} \begin{bmatrix} \widetilde{\mathbf{u}}_{\mathrm{B}} \\ \widetilde{\boldsymbol{\alpha}} \end{bmatrix} = \widetilde{\mathbf{T}}\widetilde{\mathbf{u}}, \tag{10}$$

where $\mathbf{X}_{\mathrm{st}}$ is the matrix of static modes, and $\widetilde{\mathbf{X}}$ is a reduced matrix of fixed-interface modes. The reduced substructure matrices follow as:

$$\widetilde{\mathbf{M}} = \mathbf{T}^{\mathrm{T}}\mathbf{M}\mathbf{T} \quad , \quad \widetilde{\mathbf{K}} = \mathbf{T}^{\mathrm{T}}\mathbf{K}\mathbf{T} \quad , \quad \widetilde{\mathbf{K}}'' = \mathbf{T}^{\mathrm{T}}\mathbf{K}''\mathbf{T}. \tag{11}$$

As a result, the reduced dynamic equation of the substructure writes:

$$(-\omega^2\widetilde{\mathbf{M}} + \widetilde{\mathbf{K}} + \mathrm{i}\widetilde{\mathbf{K}}'')\widetilde{\mathbf{u}} = \widetilde{\mathbf{F}}. \tag{12}$$

For substructures with parameter-dependent FE models, the reduced matrices can be obtained by matrix interpolation. The methodology stems from the strategies described in [12] and [14], whose main steps are briefly recalled hereafter. Let $\boldsymbol{\epsilon}^s$ be parameter vectors of substructures (n^s substructures), which are supposed to belong to a certain parametric space. The idea behind the proposed approach is to compute the reduced substructures matrices for some parameter vectors $\boldsymbol{\epsilon}_p$ referred to as interpolation points ($p = 1, \ldots, n^p$, with $n^p \ll n^s$). Then, let us expressed the fixed interface modes, at the interpolation points, in compatible coordinate systems as $\widehat{\mathbf{X}}_p = \widetilde{\mathbf{X}}_p(\boldsymbol{\Psi}^{\mathrm{T}}\widetilde{\mathbf{X}}_p)^{-1}$ with $\boldsymbol{\Psi} = \mathbf{M}^0_{\mathrm{II}}\widetilde{\mathbf{X}}^0$ (where superscript 0 refers to the nominal substructure, when $\boldsymbol{\epsilon}^s = \mathbf{0}$). In this case, the CB transformation matrices, at the interpolation points, writes:

$$\widehat{\mathbf{T}}_p = \begin{bmatrix} \mathbf{I} & \mathbf{0} \\ \mathbf{X}_{\mathrm{st}} & \widehat{\mathbf{X}}_p \end{bmatrix}. \tag{13}$$

Next, high-order static modes can be used to enrich the CB basis. Here, the following matrix of high-order static modes is considered [14]:

$$\mathbf{X}^{\mathrm{cor}}_{\mathrm{st}} = (\mathbf{K}^{-1}_{\mathrm{II}} - \widetilde{\mathbf{X}}\widetilde{\boldsymbol{\Lambda}}^{-1}\widetilde{\mathbf{X}}^T)(\mathbf{M}_{\mathrm{II}}\mathbf{X}_{\mathrm{st}} + \mathbf{M}_{\mathrm{IB}}), \tag{14}$$

with $\widetilde{\mathbf{\Lambda}}$ the diagonal matrix of eigenvalues associated with the retained fixed interface modes. For computational purposes, the high-order static modes can be orthogonalized through a singular value decomposition (SVD), i.e.:

$$\mathbf{X}_{\text{st}}^{\text{cor}} = \mathbf{U}\mathbf{\Sigma}\mathbf{V}^T \approx \widetilde{\mathbf{U}}\widetilde{\mathbf{\Sigma}}\widetilde{\mathbf{V}}^T, \tag{15}$$

where a reduced set of left singular vectors $\widetilde{\mathbf{U}}$ (i.e., those associated with large singular values) is only retained as enrichment vectors. Also, these vectors should can be expressed using compatible coordinate systems at the interpolation points:

$$\widehat{\mathbf{U}}_p = \widetilde{\mathbf{U}}_p((\widetilde{\mathbf{U}}^0)^T\widetilde{\mathbf{U}}_p)^{-1}. \tag{16}$$

In this case, the transformation matrices can be updated as follows (interpolation points):

$$\widehat{\mathbf{T}}_p = \begin{bmatrix} \mathbf{I} & \mathbf{0} & \mathbf{0} \\ \mathbf{X}_{\text{st}} & \widehat{\mathbf{X}}_p & \widehat{\mathbf{U}}_p \end{bmatrix}. \tag{17}$$

Within the framework of the proposed approach, the reduced substructure matrices, for any arbitrary parameter vector $\boldsymbol{\epsilon}^s$ belonging to the parametric space, can be interpolated as:

$$\widehat{\mathbf{M}}(\boldsymbol{\epsilon}^s) = \sum_{p=1}^{n^p} N_p(\boldsymbol{\epsilon}^s)\widehat{\mathbf{M}}_p, \tag{18}$$

where N_p are interpolation functions (e.g., Lagrangian polynomials). The interpolations points can be chosen as Gauss points as suggested in [14], that is $-\delta\sqrt{3/5}$, 0 and $\delta\sqrt{3/5}$ for a 1D parametric space $[-\delta\,,\,\delta]$. Once the reduced substructure matrices are obtained by interpolation, they can be classically assembled to express the reduced dynamic equation of a nearly periodic structure:

$$(-\omega^2\widehat{\mathbf{M}}(\boldsymbol{\epsilon}_a) + \widehat{\mathbf{K}}(\boldsymbol{\epsilon}_a) + \mathrm{i}\widehat{\mathbf{K}}''(\boldsymbol{\epsilon}_a)) \begin{bmatrix} (\widetilde{\mathbf{u}}_{\mathrm{B}})_a \\ \widehat{\alpha}_a \end{bmatrix} = \begin{bmatrix} (\mathbf{F}_{\mathrm{B}})_a \\ \mathbf{0} \end{bmatrix} \tag{19}$$

3.3 Interface reduction

In Eq. (19), the number of interface DOFs is usually large. In this case, an interface reduction based on the interface modes of the equivalent purely periodic structure can be proposed as in [12]. Within this framework, the interface DOFs are approximated as:

$$\begin{bmatrix} (\widetilde{\mathbf{u}}_{\mathrm{B}})_a \\ \widehat{\alpha}_a \end{bmatrix} \approx \widetilde{\mathbf{T}}_a^0 \begin{bmatrix} \widetilde{\beta}_a \\ \widehat{\alpha}_a \end{bmatrix}, \tag{20}$$

where

$$\widetilde{\mathbf{T}}_a^0 = \begin{bmatrix} \widetilde{\mathbf{X}}_a^0 & \mathbf{0} \\ \mathbf{0} & \mathbf{I} \end{bmatrix}, \tag{21}$$

and where $\widetilde{\mathbf{X}}_a^0$ is a reduced set of eigenvectors of the matrix pencil $((\mathbf{K}_{\mathrm{BB}})_a^0, (\mathbf{M}_{\mathrm{BB}})_a^0)$, which is associated with the equivalent purely periodic structure ($\boldsymbol{\epsilon}^s = \mathbf{0}$ for all the substructure). Then, the following reduced dynamic equation of the nearly periodic structure can be obtained:

$$\left[-\omega^2[(\widetilde{\mathbf{T}}_a^0)^T\widehat{\mathbf{M}}(\boldsymbol{\epsilon}_a)(\widetilde{\mathbf{T}}_a^0)] + [(\widetilde{\mathbf{T}}_a^0)^T\widehat{\mathbf{K}}(\boldsymbol{\epsilon}_a)(\widetilde{\mathbf{T}}_a^0)] + \mathrm{i}[(\widetilde{\mathbf{T}}_a^0)^T\widehat{\mathbf{K}}''(\boldsymbol{\epsilon}_a)(\widetilde{\mathbf{T}}_a^0)\right] \begin{bmatrix} (\widetilde{\mathbf{u}}_{\mathrm{B}})_a \\ \widehat{\alpha}_a \end{bmatrix} = (\widetilde{\mathbf{T}}_a^0)^T \begin{bmatrix} (\mathbf{F}_{\mathrm{B}})_a \\ \mathbf{0} \end{bmatrix}. \tag{22}$$

4 NUMERICAL RESULTS

Numerical results are proposed in this section, focused on the dynamic analysis of plates with 5×3 periodic and nearly periodic arrays of ABH substructures. Substructures of size 0.3×0.3 m^2 and nominal thickness h_0=2 mm, made of steel material (Young's modulus E=210 GPa, Poisson's ratio ν=0.3, density ρ=7860 kg.m^{-3}), are considered. In this case, each substructure embeds an ABH those properties are: quadratic thickness profile (m=2), radius R=0.1 m, minimum thickness $h_{\min}$=50 μm. Each ABH is covered by a damping layer with the following properties: Young's modulus E_l=7 GPa, Poisson's ratio ν=0.3, density ρ_l=1000 kg.m^{-3}, loss factor η_l=0.2, thickness h_l=0.1 mm, and radius R_l=0.05 m. A local mass (nominal value $m^s = m^0$ =10 g) is added to the center of each ABH substructure. Near-periodicity is taken into account by perturbating the local mass m^s of the substructures. The FE mesh of an ABH substructure is shown in Fig. 2(a). Also, the thickness profile of the substructure is displayed in Fig. 2(b), and the schematic of the plate with the ABH array is shown in Fig. 2(c). Here, the red cross and the red dot indicate the excitation and measurement points, respectively, which will be used to obtain the response functions of the structure.

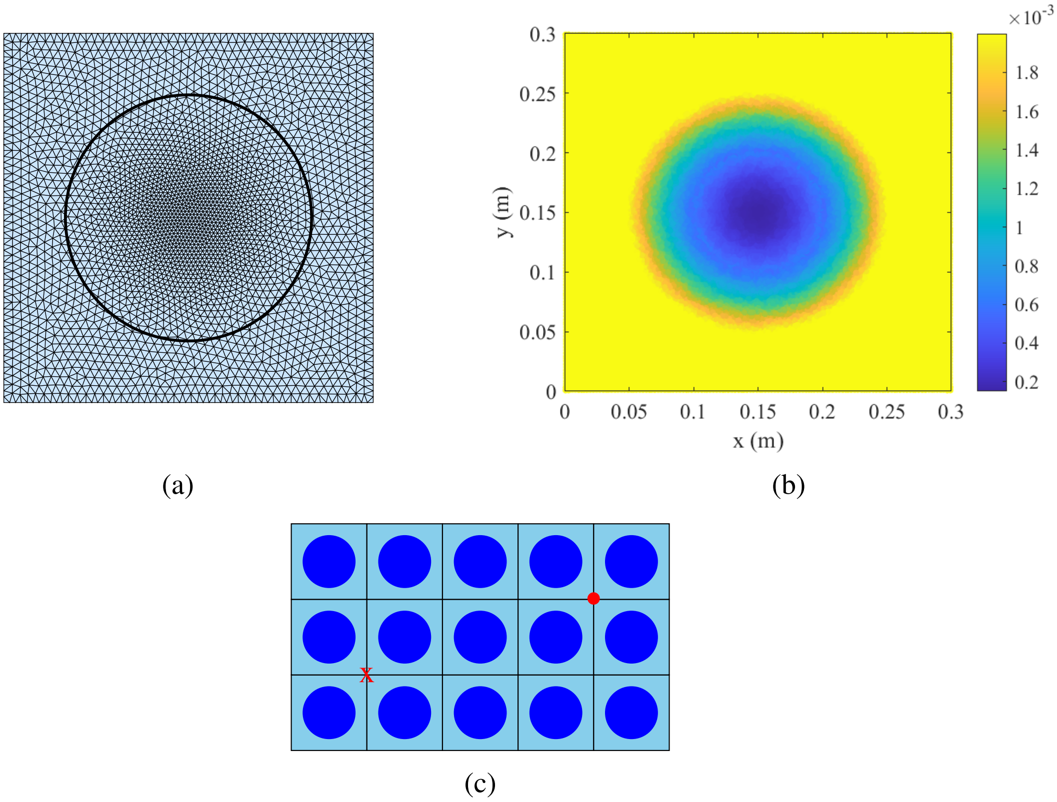

Figure 2: (a) FE mesh of the ABH substructure, (b) thickness profile of the ABH substructure, and (c) schematic of the plate with a 5×3 array of circular ABHs.

4.1 Validation of the model reduction strategy

In this section, the proposed model reduction strategy (see Sec. 3) is used to predict the frequency response functions (FRFs) of the plate with the ABH array and different local masses

m^s. For every substructure $s \equiv (i, j)$ corresponding to a row i ($i = 1, 2, 3, 4, 5$) and a column j ($j = 1, 2, 3$), the local masses are:

$$[m^s]_{ij} = \begin{bmatrix} 11 & 10 & 9 & 12 & 11 \\ 10 & 8 & 15 & 13 & 7 \\ 11 & 11 & 10 & 7 & 8 \end{bmatrix} \text{ g.} \tag{23}$$

Within the proposed strategy, three interpolation points (1D parametric space) are considered, which are associated with m^s =5 g, m^s =10 g and m^s =15 g. In Fig. 3, the FRFs of the nearly periodic structure (without damping layer) is plotted and compared with a standard reference solution issued from the full order model (FOM) of the structure, over the $[0\,,\,2000]$ Hz range (4000 points). Concerning the proposed strategy, 100 fixed interface modes and 20 high-order static modes are used to model the substructures, and 350 interface modes (interface reduction) are used. These results show that the proposed approach is in excellent agreement with the FOM solution, not only in the low frequency range (see next subsections), but also in the high frequency range. This fully validates the proposed approach, including the CB reduction of the substructures, the matrix interpolation strategy, and the interface reduction. In this case, it takes 5200 s to compute the FRF with the FOM on $[0\,,\,2000]$ Hz, against 760 s with the model reduction strategy. Overall, this yields a reduction of 85% of the computational times. Here, a moderately high number of fixed interface modes, enriched with a few high-order static modes, has been used to obtain accurate results with the interpolation strategy in the band gap region (low frequency range), as well as in the high frequency range (see [14]). Also, a moderately high number of interface modes has been used to compute accurate FRFs in the high frequency range.

4.2 Dynamic behavior of the plate with a periodic array of ABH substructures

In this section, FRFs of the plate with a periodic array of ABH substructures are discussed. Four cases are studied, which concern ABHs without and with damping layers, and without and with central masses. The results are shown in Figs. 4 and 5. Concerning the undamped case with central masses (Fig. 4(a)), we may notice a narrow band gap around 39 Hz that correspond to the band gap previously identified in Fig. 1 (Sec. 2.2). Regarding Fig. 4(b), it is seen that the damping layer effect strongly reduces the vibration levels on some frequency bands. Indeed, adding central masses to an array of damped ABHs creates a region with reduced vibration levels in the range where the ABH is not efficient. Compared to the undamped case, the band gap can be spread at high frequencies to cover a wide frequency region, say $[39\,,\,70]$ Hz. FRF results on $[0\,,\,2000]$ Hz for undamped and damped ABHs with local masses are shown in Fig. 5(a). The ABH effect comes into play after a given cut-on frequency (about 400 Hz in this case), where it is seen that the use of damped ABHs allows the resonant behavior of the structure to be strongly reduced [15].

4.3 Dynamic behavior of the plate with a nearly periodic array of ABH substructures

In this section, ABH substructures subjected to variations of the local masses m^s are considered, where m^s represent independent random variables that are supposed to follow a uniform distribution on $[5\,,\,15]$ g. Preliminary results about undamped ABHs with mass variations have been given in Fig. 3, where it is seen that the near periodicity can strongly affect the band gap effect (periodic case), in the sense that a series of peaks is generated in this region. In order to discuss this result, a Monte Carlo (MC) analysis can be performed. MC simulations can

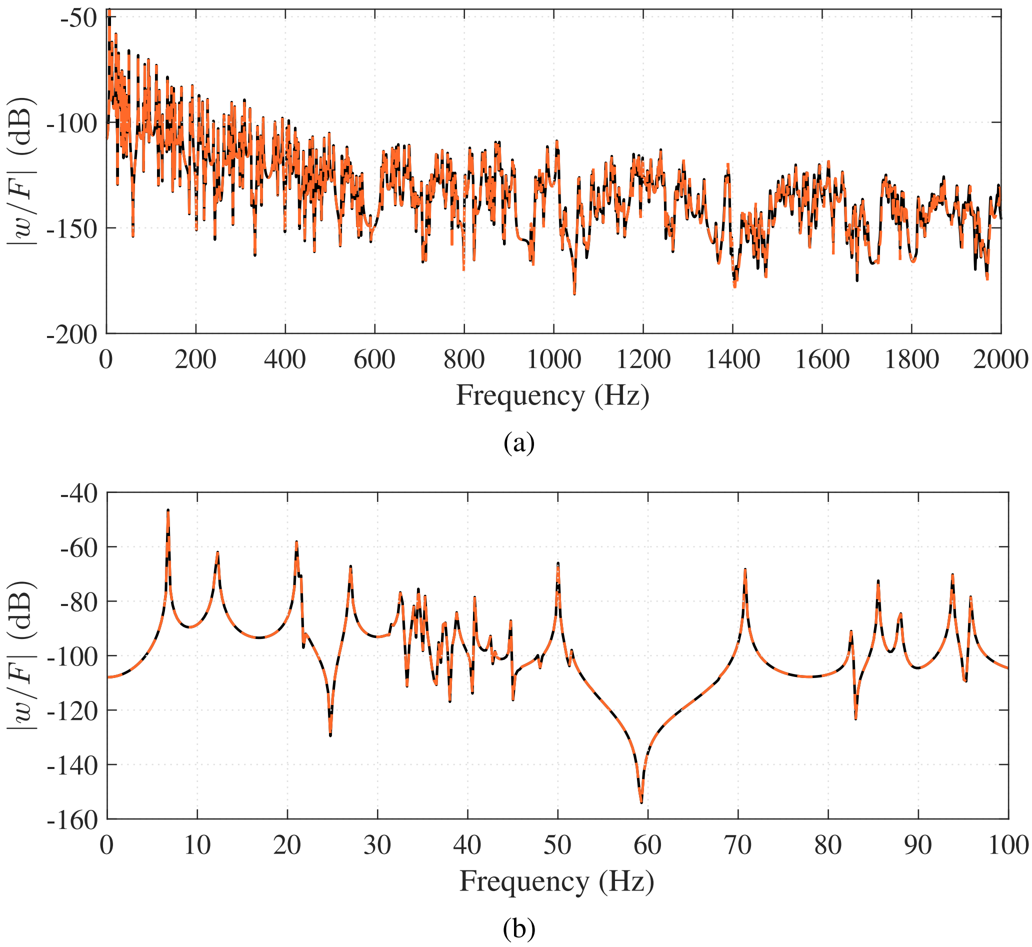

Figure 3: FRF of the nearly periodic plate with ABH substructures: (a) FOM (black solid line) and interpolation strategy (red dashed line); (b) zoom of the FRFs on $[0\,,\,100]$ Hz.

be achieved at affordable computational times using the proposed interpolation strategy. In this case, it takes 3h30 to compute the FRFs of the nearly periodic structures for 20 different mass configurations, on $[0\,,\,2000]$ Hz. Results about ABHs without damping layer are shown in Fig. 6, where the range of variability of the FRF solutions is displayed in purple shaded area. Also, in Fig. 6, the FRF of the purely periodic structure is shown in black solid line. Fig. 6(a) shows that the near periodicity does not affect the FRF of the periodic structure, except around the resonant band gap. A closer look of the FRFs on $[0\,,\,100]$ Hz is proposed in Fig. 6(b), which indicates that the dynamic response is very sensitive to the variability of the added mass around the band gap region (periodic case). This also shows that the FRFs of the nearly periodic structures do not reveal a clear band gap phenomenon (i.e., as opposed to periodic structures). MC simulations about damped ABHs with mass variations are also performed, see Fig. 7. Here, the FRFs also show strong dispersion in the band gap region, and overall low vibration levels without sharp resonance peaks. Importantly, the frequency region corresponding to these low vibration levels does not seem to be affected by the near periodicity. It can be concluded that damped arrays of nearly periodic ABH substructures constitutes robust designs able to provide reliable solutions about the vibration reduction in structures.

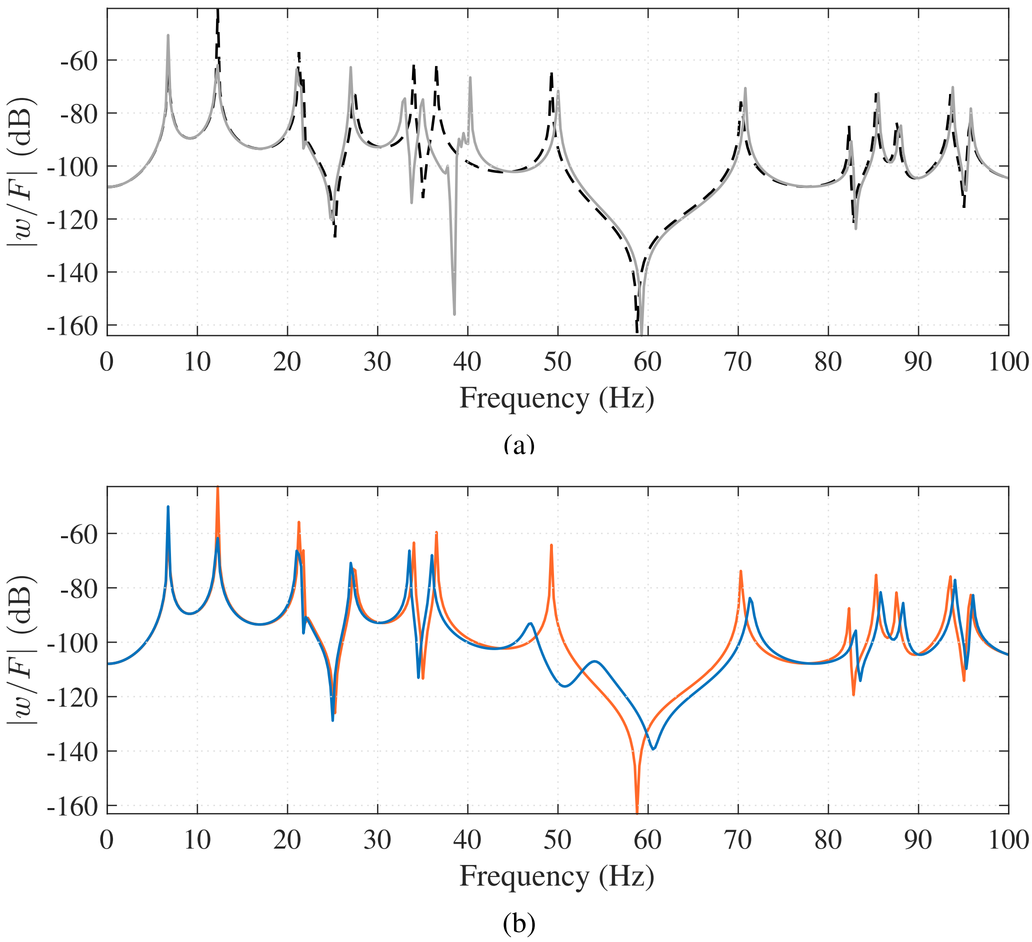

Figure 4: FRF of the periodic structure on $[0\,,\,100]$ Hz: (a) ABH without damping layer, without central mass (black dashed line) and with central mass (gray solid line); (b) ABH with damping layer, without central mass (orange solid line) and with central mass (blue solid line).

5 CONCLUSION

The dynamic behavior of plates with periodic and nearly periodic arrays of ABHs has been investigated. A model reduction strategy has been proposed. Within this framework, the reduced CB matrices of ABH substructures subjected to parametric changes can be easily obtained by interpolation. To improve the accuracy of the CB bases of the substructures, they can be enriched with high-order static modes. Also, an interface reduction (between the substructures) can be considered to speed up the computation of the dynamic equation of a whole periodic or nearly periodic structure. Numerical results have been proposed concerning periodic arrays of ABHs with local masses, which have shown that low frequency band gaps can be created. The presence of a damping layer (ABH) can significantly enlarge the band gap region, which appears promising in the vibration control of structures. For nearly periodic structures involving undamped ABH arrays with mass variability, a clear band gap effect cannot be highlighted. In the damped case, band gap occurs in the form of a wide spread frequency region of low vibration levels. MC simulations have shown that this band gap region is weakly sensitive to the mass variability. Also, it has been shown that, in the damped and undamped cases, the near periodicity does not affect the FRFs of the structure at high frequencies. Further works

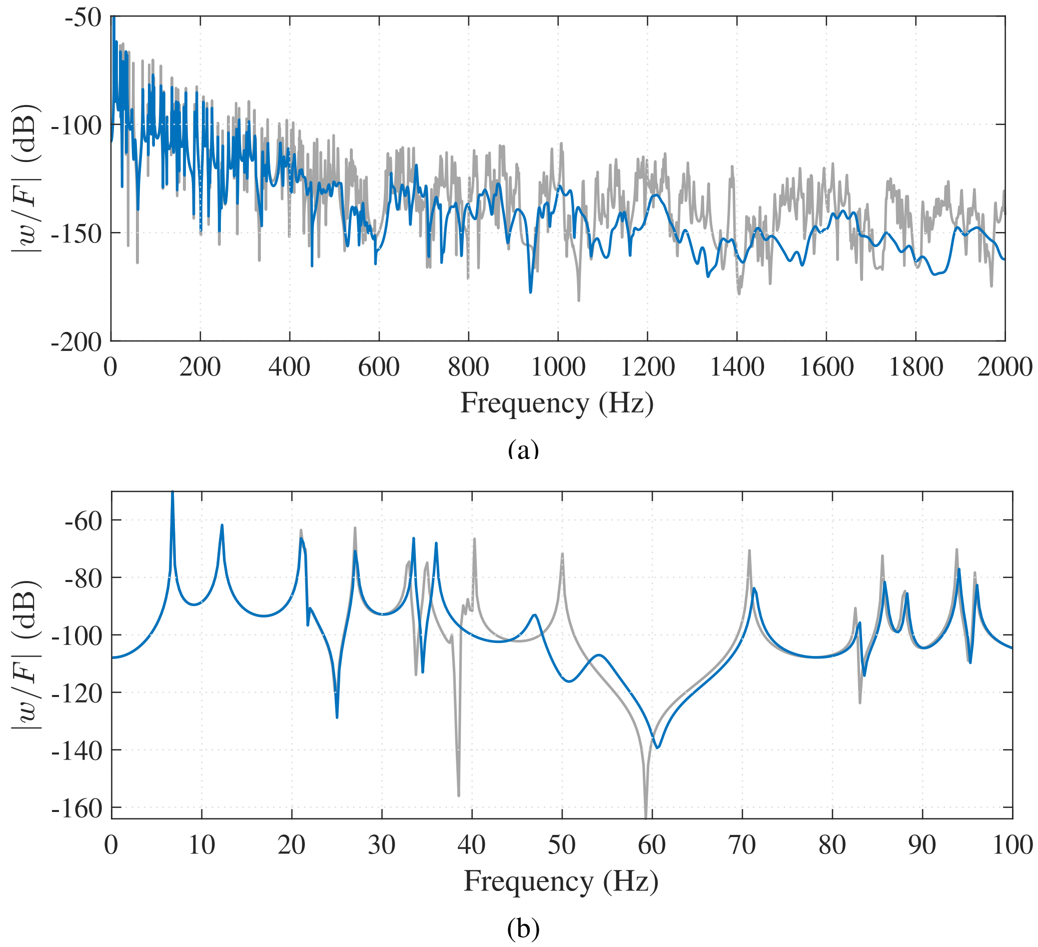

Figure 5: FRF of the periodic structure on $[0\,,\,2000]$ Hz (a) and $[0\,,\,100]$ Hz (b): (gray solid line) ABH without damping layer and with central mass (gray solid line); (blue solid line) ABH with damping layer and with central mass (blue solid line).

in this topic could include the analysis of nearly periodic structures containing more complex parameter-dependent ABH substructures, e.g., considering variations of the minimum thickness of the ABHs, or more complex geometric changes.

REFERENCES

[1] M.A. Mironov. Propagation of a flexural wave in a plate whose thickness decreases smoothly to zero in a finite interval. *Soviet Physics:Acoustics*, 34(3):318–319, 1988.

[2] V. V. Krylov. New type of vibration dampers utilising the effect of acoustic 'black holes'. *Acta Acustica united with Acustica*, 90(5):830–837, 2004.

[3] H. Zhu and F. Semperlotti. Phononic thin plates with embedded acoustic black holes. *Physical Review B*, 91(10):104304, 2015.

[4] O. Aklouche. *Réduction des niveaux vibratoires d'un panneau au moyen de trous noirs acoustiques structurés en réseau périodique : conception d'une méta-plaque*. PhD thesis, Le Mans, 2017.

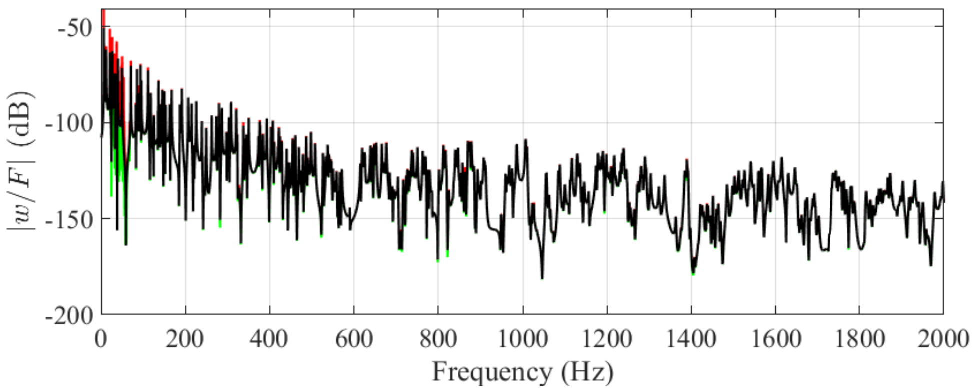

(a)

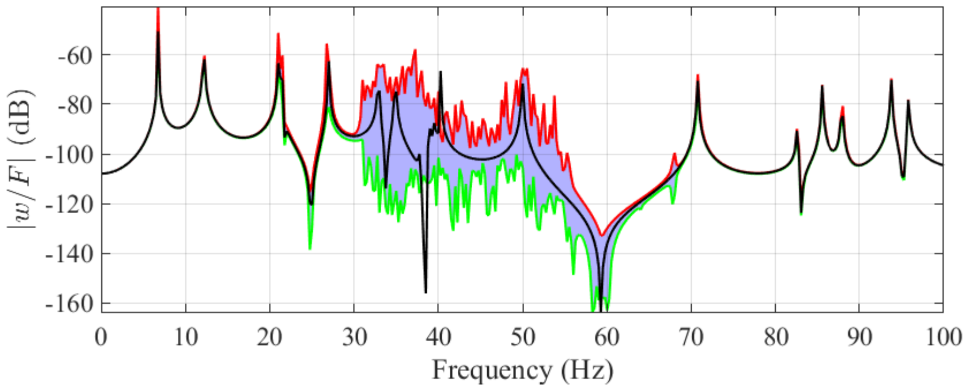

(b)

Figure 6: FRF of the nearly periodic structure (ABH without damping layer) on $[0\,,\,2000]$ Hz (a) and $[0\,,\,100]$ Hz (b): (black solid line) periodic structure; (green and red lines) lower and upper bounds (MC simulations).

[5] L. Tang and L. Cheng. Ultrawide band gaps in beams with double-leaf acoustic black hole indentations. *The Journal of the Acoustical Society of America*, 142(5):2802–2793, 2017.

[6] L. Tang and L. Cheng. Periodic plates with tunneled Acoustic-Black-Holes for directional band gap generation. *Mechanical Systems and Signal Processing*, 133:106257, November 2019.

[7] L. Zhao. Low-frequency vibration reduction using a sandwich plate with periodically embedded acoustic black holes. *Journal of Sound and Vibration*, 441:165–171, February 2019.

[8] J. Deng, N. Gao, X. Chen, B. Han, and H. Ji. Evanescent waves in a metabeam attached with lossy acoustic black hole pillars. *Mechanical Systems and Signal Processing*, 191:110182, May 2023.

[9] J. Deng, Y. Xu, O. Guasch, N. Gao, L. Tang, and X. Chen. A two-dimensional wave and Rayleigh–Ritz method for complex dispersion in periodic arrays of circular damped

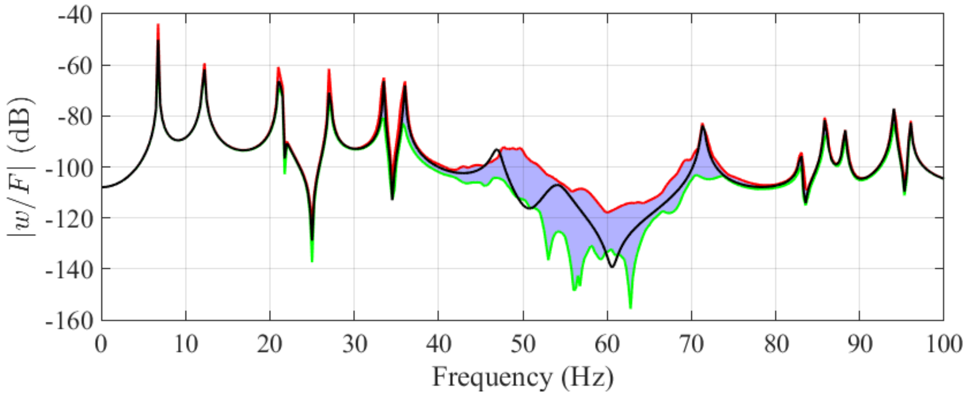

Figure 7: FRF the nearly periodic structure (ABH with damping layers) on $[0\,,\,100]$ Hz: (black solid line) periodic structure; (green and red lines) lower and upper bounds (MC simulations).

acoustic black holes. *Mechanical Systems and Signal Processing*, 200:110507, October 2023.

[10] B. Han, H. Ji, L. Cheng, W. Huang, and J. Qiu. Attenuation band splitting in a finite plate strip with two-dimensional acoustic black holes. *Journal of Sound and Vibration*, 546:117442, March 2023.

[11] M. C. C. Bampton and R. R. Craig, Jr. Coupling of substructures for dynamic analyses. *AIAA Journal*, 6(7):1313–1319, July 1968.

[12] J.-M. Mencik. Model reduction based on matrix interpolation and distorted finite element meshes for dynamic analysis of 2D nearly periodic structures. *Finite Elements in Analysis and Design*, 188:103518, June 2021.

[13] H. Panzer, J. Mohring, R. Eid, and B. Lohmann. Parametric model order reduction by matrix interpolation. *at-Automatisierungstechnik*, 58(8):475–484, 2010.

[14] J.-M. Mencik. Improved model reduction with basis enrichment for dynamic analysis of nearly periodic structures including substructures with geometric changes. *Journal of Computational and Applied Mathematics*, 445:115844, August 2024.

[15] V. Denis, A. Pelat, F. Gautier, and B. Elie. Modal Overlap Factor of a beam with an acoustic black hole termination. *Journal of Sound and Vibration*, 333(12):2475–2488, 2014.

[16] V. Denis, A. Pelat, C. Touzé, and F. Gautier. Improvement of the acoustic black hole effect by using energy transfer due to geometric nonlinearity. *International Journal of Non-Linear Mechanics*, 94(November 2016):134–145, 2017.

[17] J.-L. Batoz and G. Dhatt. *Modélisation des Structures par Éléments Finis, Volume 1: Solides élastiques; Volume 2: Poutres et plaques; Volume 3: Coques, Editions Hermes, Paris*, volume 37. 1994.

[18] P.-O. Persson and G. Strang. A Simple Mesh Generator in MATLAB. *SIAM Review*, 46(2):329–345, January 2004.